Electronic Supplementary Material (ESI) for New Journal of Chemistry.
This journal is © The Royal Society of Chemistry 2014

Electronic Supplementary Information

Heterometallic complexes combining $[Mn^{III}(salpn)]^{+}$ and $[Fe(CN)_6]^{4-}$ units as the products of reactions between $[Mn^{III}(salpn)(H_2O)C(CN)_3]$ and $[Fe(CN)_6]^{3-/4-}$

Vyacheslav A. Kopotkov,[a*] Eduard B. Yagubskii,[a*] Sergey V. Simonov,[b] Leokadiya V. Zorina,[b*] Denis V. Starichenko,[c] Alexander V. Korolyov,[c] Vladimir V. Ustinov[c] and Yurii N. Shvachko[c,d*]

[a] *Institute of problems of Chemical Physics, Chernogolovka, Moscow District, Academician Semenov av. 1, 142432 Russian Federation. E-mail: yagubski@icp.ac.ru; Fax: +7 496-5225636; Tel: +7 495-9935707*

[b] *Institute of Solid State Physics, Chernogolovka, Moscow District, Academician Ossipyan str. 2, 142432 Russian Federation. E-mail: zorina@issp.ac.ru; Fax: +7 496-5228160; Tel: +7 496-5221982*

[d] *Institute of Metal Physics, S. Kovalevskaya st. 18, 620990 Ekaterinburg, Russian Federation. Fax: +7 343-3745244; Tel: +7 343-3740230*

[d] *Department of Mathematics, University of California, Davis, CA 95616, USA. E-mail: yshvachko@ucdavis.edu; Fax: +7 343-3745244; Tel: +7 343-3740230*

Crystal structures

$[\{Mn(salpn)(H_2O)\}_2\{Mn(salpn)(H_2O)_{0.7}(CH_3OH)_{0.3}\}_2Fe(CN)_6]n\cdot(H_2O/CH_3OH)$ (2).

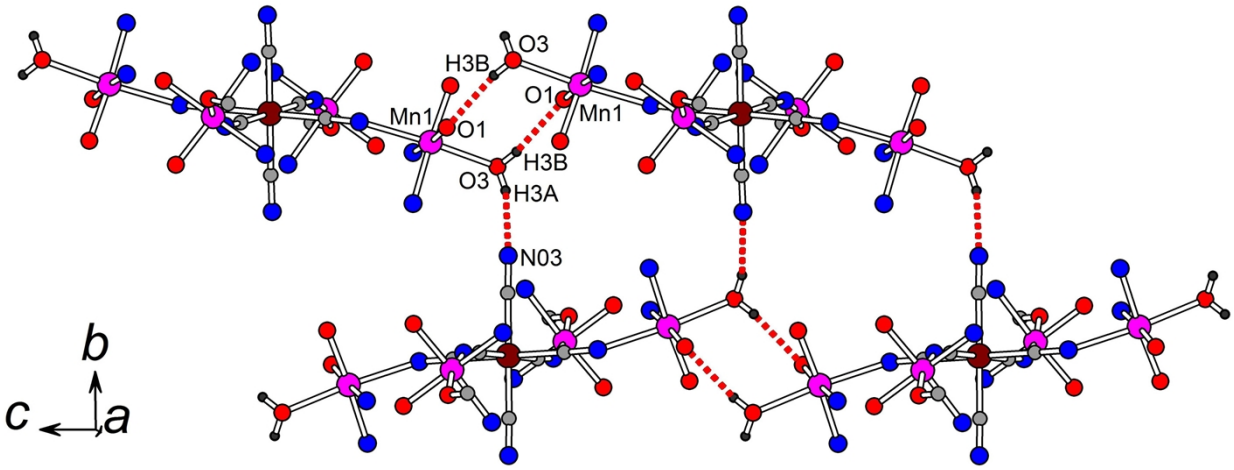

Figure S1. Packing diagram and hydrogen bonding within the *bc* layer in the structure of **2**. The non-coordinated atoms of salpn ligand are omitted for clarity. Geometry of hydrogen D-H…A bonds (H…A, D-A distances and D-H…A angle): O3-H3B…O1 2.16, 2.914(3) Å, 159.5(1)º; O3-H3A…N03 2.06, 2.815(4) Å, 163.2(1)º.

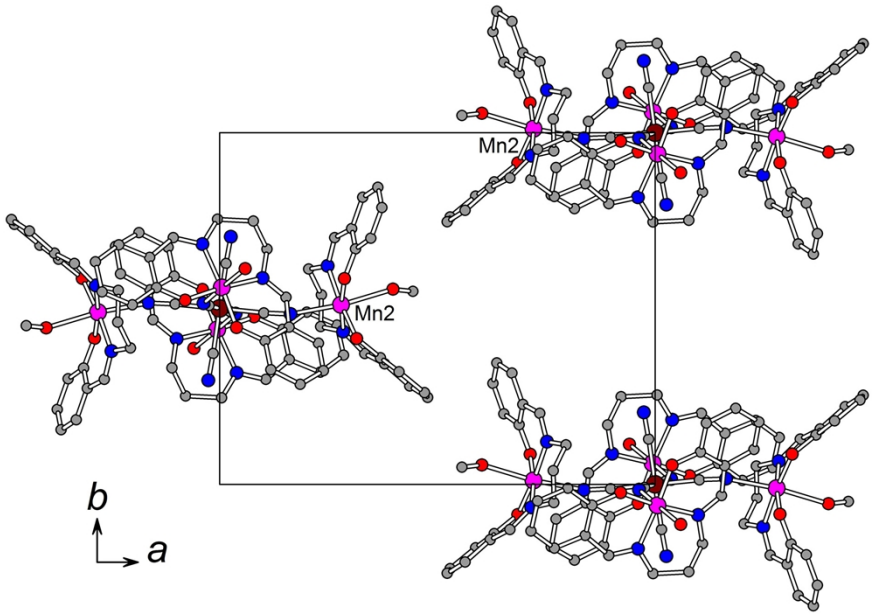

Figure S2. Packing mode of adjacent *bc* layers in **2**.

[{Mn(salpn)}$_4${Mn(salpn)(H$_2$O)}$_2$Fe(CN)$_6$]{C(CN)$_3$}$_2$·4H$_2$O (3).

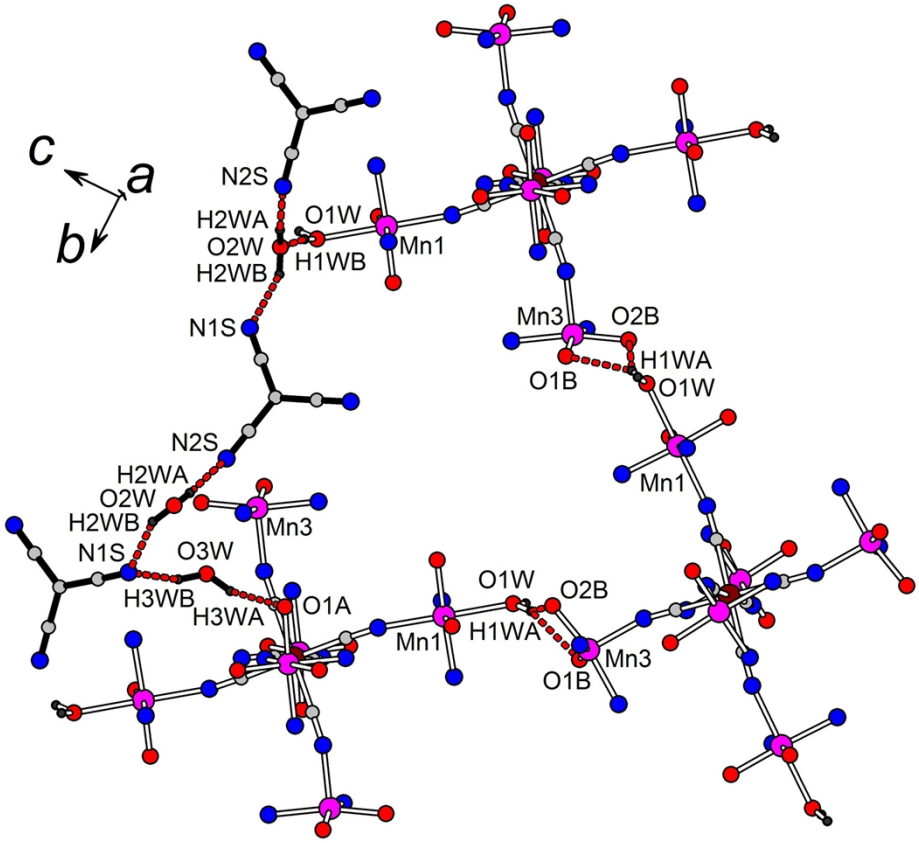

Figure S3. Hydrogen bonding in **3**. H…O and H…N contacts are shown by red dashed lines, the non-coordinated atoms of salpn ligands are omitted for clarity. Geometry of hydrogen D-H…A bonds (H…A, D-A distances and D-H…A angle): O1W-H1WA…O1B 2.32, 3.108(3) Å, 145.7(2)º; O1W-H1WA…O2B 2.31, 3.115(4) Å, 148.4(2)º; O1W-H1WB…O2W 1.89, 2.782(4) Å, 172.4(2)º; O2W-H2WA…N2S 2.10, 2.996(5) Å, 173.8(2)º; O2W-H2WB…N1S 2.16, 2.965(6) Å, 148.3(2)º; O3W-H3WA...O1A 2.03, 2.939(7) Å, 155.1(4)°; O3W-H3WB...N1S 1.96, 2.861(9) Å , 154.5(4)°.

Additional structure refinement details for 2:

In **2**, salpn moiety of the Mn(2) unit is disordered between two positions with nearly 2/3 and 1/3 occupancies related by ~25º rotation about $N_{cyanido}$-Mn2 axis (Fig. S4). Propylene group of another salpn is disordered between two sites of 0.6/0.4 occupancy. Only major positions are shown in Figures 1 and S2. Non-coordinated water and methanol molecules were not localized in **2** and their contribution into electronic density was subtracted by PLATON/SQUEEZE procedure; two free cavities of 118 $Å^3$ per unit cell, each containing 29e, were found. After SQUEEZE, only three partially occupied water sites were localized near disordered salpn units and included into refinement.

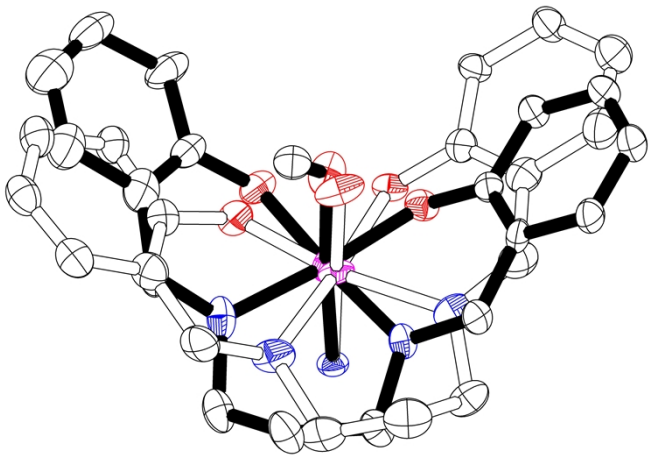

Figure S4. Molecular disorder of the $\{Mn^{III}(salpn)(H_2O)_{0.7}(CH_3OH)_{0.3}\}$ moiety in the complex **2** (30% ellipsoid probability, H-atoms are omitted for clarity, black bonds are drawn for major position with ~2/3 occupancy).

Numerical simulations of the magnetic susceptibility of 3.

The calculated values of spin susceptibility for four magnetic moments S=2 with g=1.94 and several D_{PM} parameters from 0 to -2.0 cm^{-1} ($4\chi_p$(T)) were subtracted from the experimental χ(T) data points for **3**. In fact, the *D*-parameters for the ions in square pyramidal Mn(3), Mn(3**) co-ordinations could be omitted. We did calculations both for two and for four D_{PM} parameters. The resulting datasets are presented in Fig. S5, as orange (D=0 cm^{-1}), blue (D=-0.50 cm^{-1}) and green (D=-1.00 cm^{-1}) circles. The obtained points were simulated by using the Heisenberg–Van Vleck model for the exchange-coupled dimer with two independent parameters: *D* and *J*. The *g*-factor was set 1.94. The plot indicates that ZFS parameters for the paramagnetic Mn^{III} moments do not affect the total magnetic susceptibility above 5 K in the reasonable range of *D*.

A good fit in the range 10 K<T<300 K was obtained at J=0.64 cm^{-1} for all $|D| \leq 4.0$ cm^{-1}. On contrary, at temperatures T<10 K the better agreement required higher values of $|D|$. The acceptable fitting was found for D=-8.0 cm^{-1}, which is beyond reasonable values and ruins agreement at higher temperatures.

On the next step, we varied *J* parameter while the *D* values were fixed. In the Fig. S6 we show that even 15% change of *J* immediately induces an unacceptable discrepancy at T>10 K.

Thus, the value of J=0.64 cm^{-1} was determined with good accuracy. A compromise solution for *D* parameter over the entire temperature range was reached at -4.0<D<-3.0, *i.e.* D=-3.5±0.5 cm^{-1}.

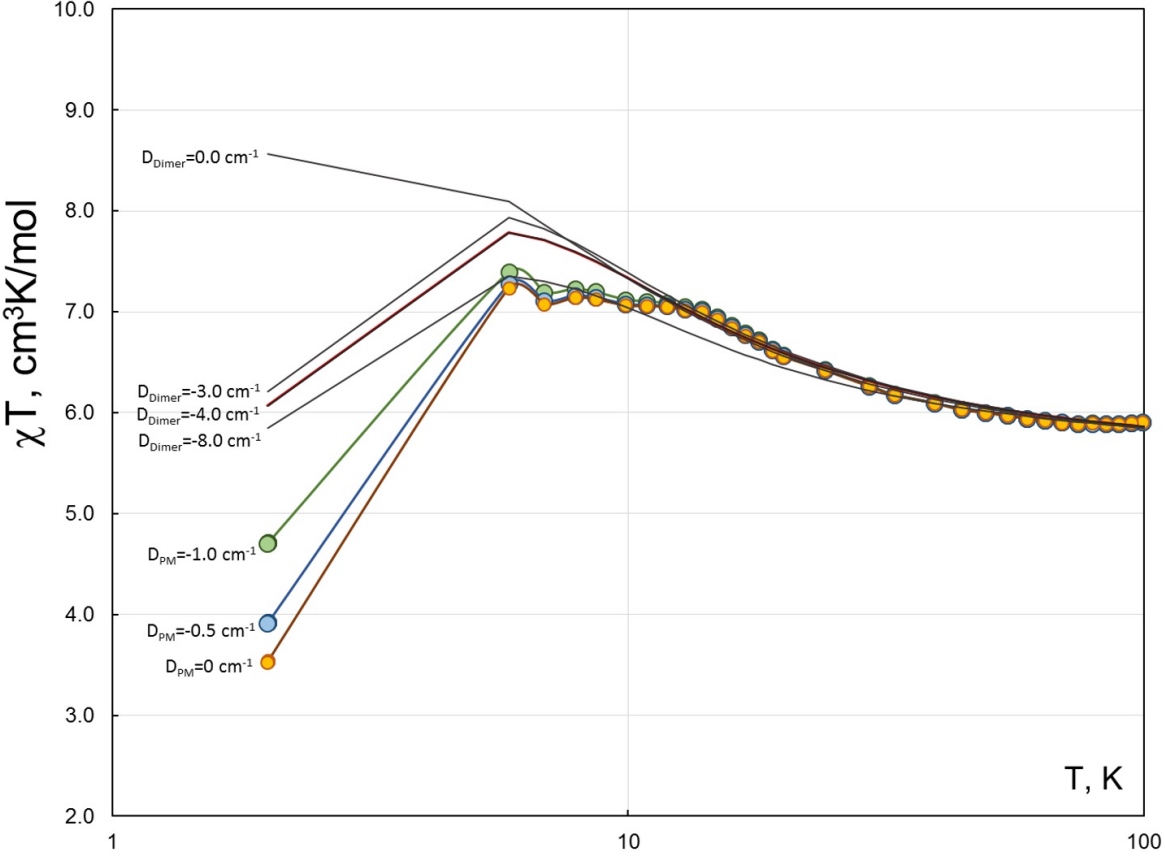

Figure S5. Dimer contribution to the magnetic susceptibility extracted from the experiment by subtraction of the paramagnetic response of 4 S=2 moments with various *D*: orange (*D*=0 cm^{-1}), blue (*D*=-0.5 cm^{-1}) and green (*D*=-1.0 cm^{-1}). Solid dark lines are fittings by the Heisenberg–Van Vleck model with *J*=0.64 cm^{-1} and *D*=0; -3.0; -4.0; -8.0 cm^{-1}.

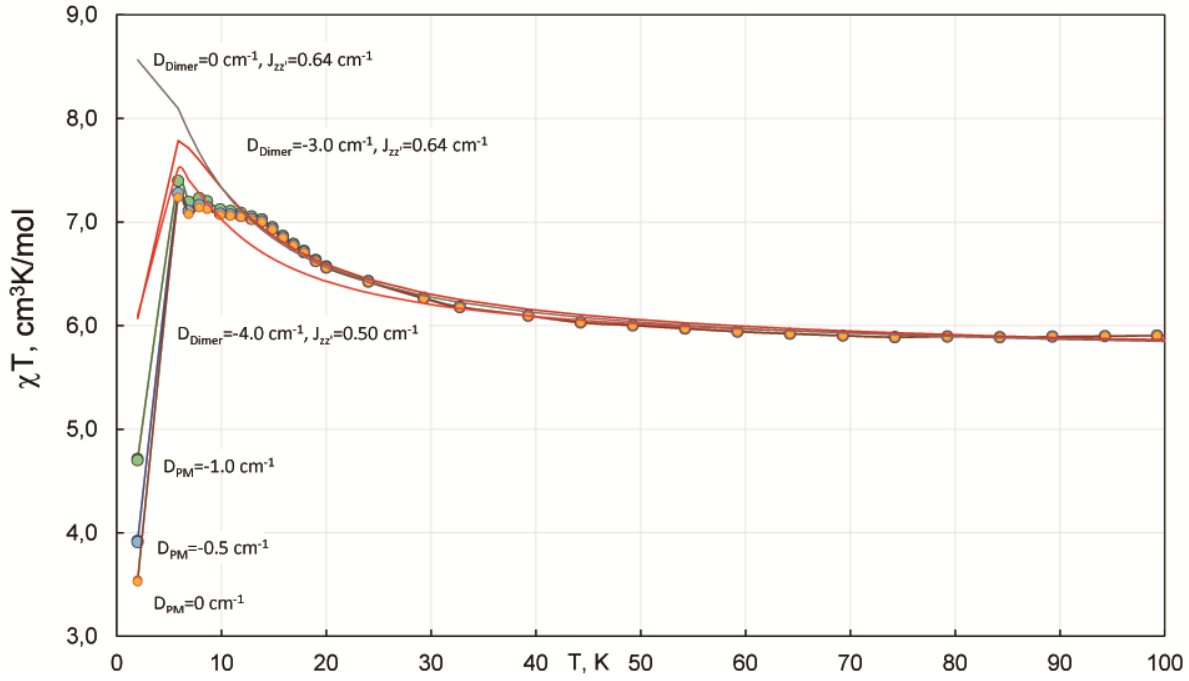

Figure S6. Comparison of the simulations of the dimer contribution to the magnetic susceptibility by variation of *J*: red line - *J*=0.50 cm^{-1} compare to dark-red 0.64 cm^{-1}. Difference between grey line (*D*=0 cm^{-1}) and dark-red line (*D*=-3.0 cm^{-1}) shows magnitude of variation of the χT product while changing *D* parameter.